Supplemental Information

Chokepoints in Mechanical Coupling Associated with Allosteric Proteins: The Pyruvate Kinase Example

Lewis E. Johnson, Bojana Ginovska, Aron W. Fenton, and Simone Raugei

Validation of cutoff distances for local correlation

One of the key parameters in building the local correlation graph underlying the **M**-matrix is the cutoff distance between residues (R_{cut}) beyond which residues are considered to be non-interacting. If this distance is set too short, strong non-covalent interactions between side chains may be ignored, but if it is set too long, residues that are identified as interacting may not be interacting directly, with their interactions instead mediated by a third residue. For the method to function optimally, it should include **all** pairwise correlations, and **only** pairwise correlations. Previous work [1-2] by Dokholyan and co-workers found that an inter-residue distance of 7.5 Å provided a reasonable cutoff. Increasing R_{cut} to 10 Å (Figure S1) results in a much higher density of paths, likely including some non-local correlations, while reducing R_{cut} to 5 Å (Figure S1) leaves a very sparse graph that only includes the strongest correlations. Reducing below 5 Å results in some isolated nodes (residues not indicated as interacting with any other residues).
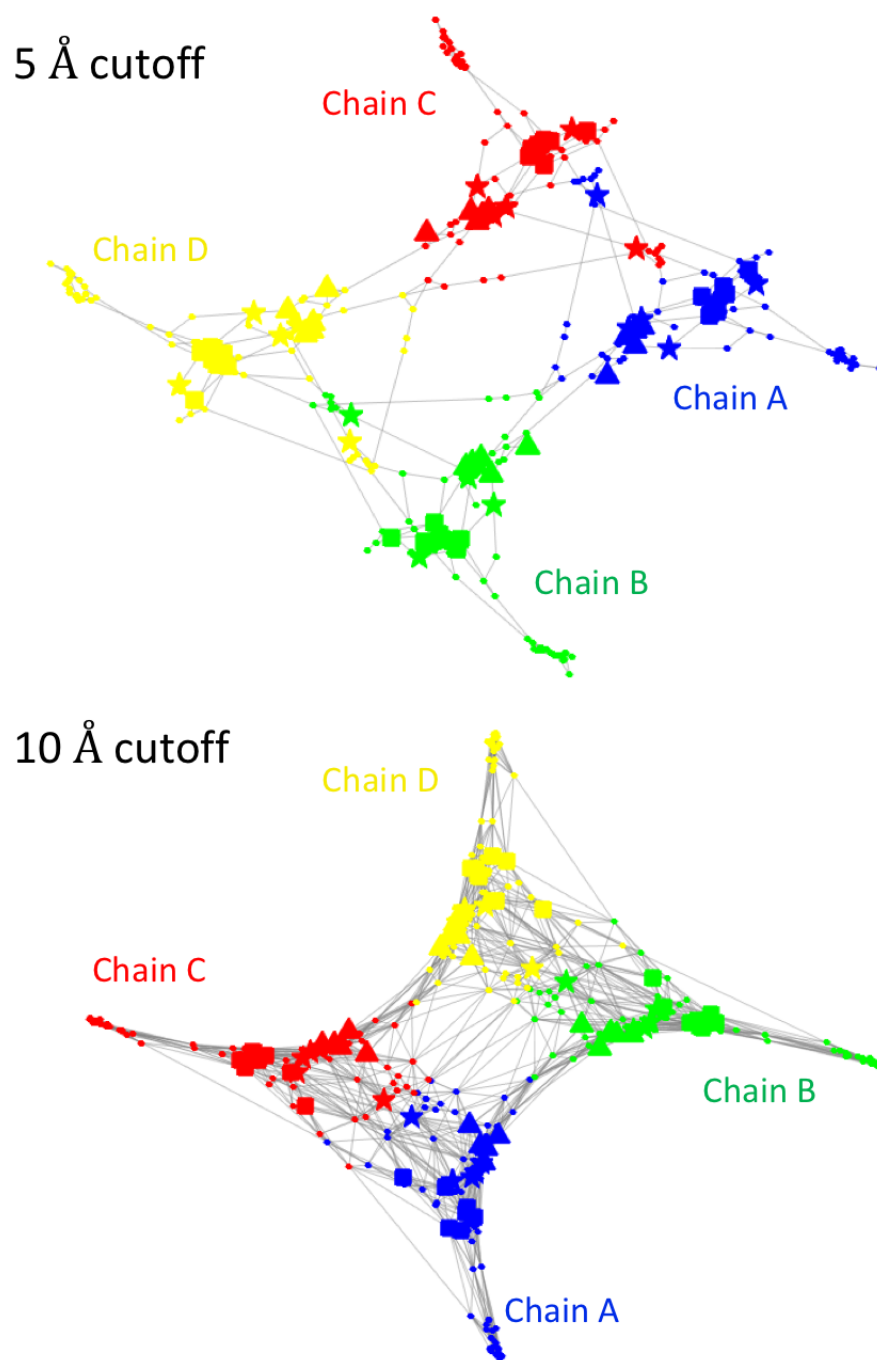
Figure S1. Mechanical coupling graphs for human liver pyruvate kinase using Euclidian distance cutoffs R_{cut} for building the adjacency matrix. Chains are distinguished by color; PEP sites are shown as squares, FBP sites as triangles, and Ala[E] sites as stars. Reducing the cutoff reduces the density of possible paths, though the essential configuration of the protein is preserved.

Effects of crystal structure symmetrization

A number of residues were absent or poorly resolved in the source crystal structure for hL-PYK (PDB: 4IMA). Missing or poorly resolved residues were not consistent between the four chains in the hL-PYK homotetramer, translating to an asymmetric mechanical coupling graph (Figure S2, left). The asymmetries were resolved by reconstructing the protein from applying symmetry operations to the structure of chain A to build a nearly complete, symmetric model. While differences could easily be visually resolved in the graph, effects on the M-matrix and χ parameters were minimal and were primarily localized to chain D, which had the most unresolved residues (83 out of 543, vs 21 for chain A). The non-symmetrized M-matrix for 4IMA in terms of secondary structural elements is shown in Figure S2, right.
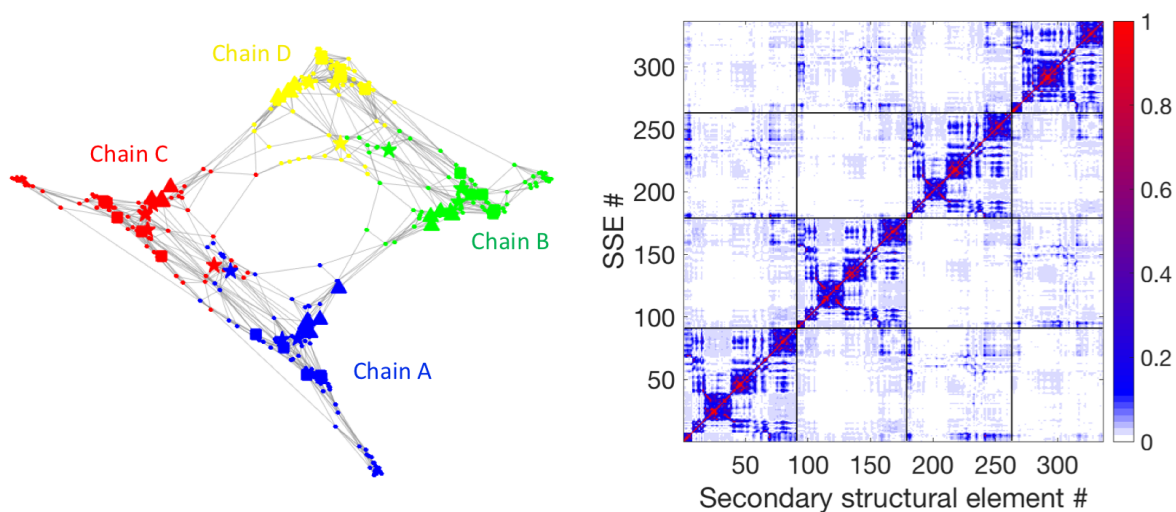
Figure S2. Non-symmetrized mechanical coupling graph for 4IMA (left) and corresponding M-matrix (right)

4

Reduced D, C, G, and P-matrices for hL-PYK

Graphs shown in the main manuscript have been reduced to secondary structural elements for clarity in illustrating and understanding mechanical couplings. As the residues within each secondary structural element are strongly coupled to each other, coarse-graining the structure from residues to secondary structural elements does not have any substantial qualitative effect on the interactions shown by the **C** (Figure S3, top right) and **M** matrix (Figure S3, bottom right), along with the Euclidian distance matrix **D** (Figure S3, top left) used for deriving the graph and geodesic **G** (Figure S3, bottom left) distance matrix for the graph that is used to derive the **M**-matrix.
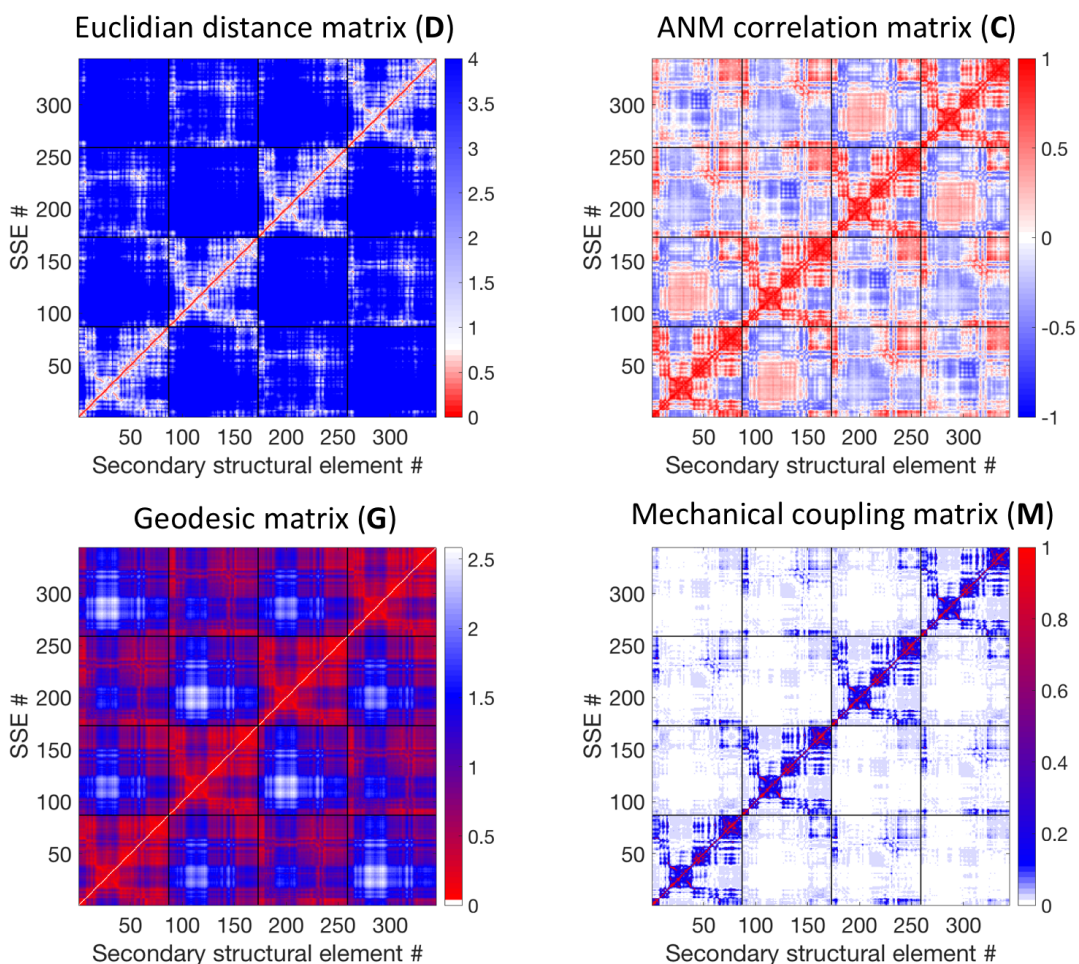
Figure S3. Reduced Euclidian distance (D, **top left**) correlation (C, **top right**), geodesic distance (G**, bottom left**) and mechanical coupling (M, **bottom right**) matrices for hL-PYK, crystal structure 4IMA.

Example shortest path tree

Shortest path trees are a type of subgraph that represents the geodesic path from one node i on a graph to every other node $j{\neq}i$ on the graph. The betweenness centrality metric for evaluating coupling between sites uses a subgraph built from residues that are identified as of interest based on the **M**-matrix and/or experimental data. An example of a shortest path tree is shown in Figure S4.
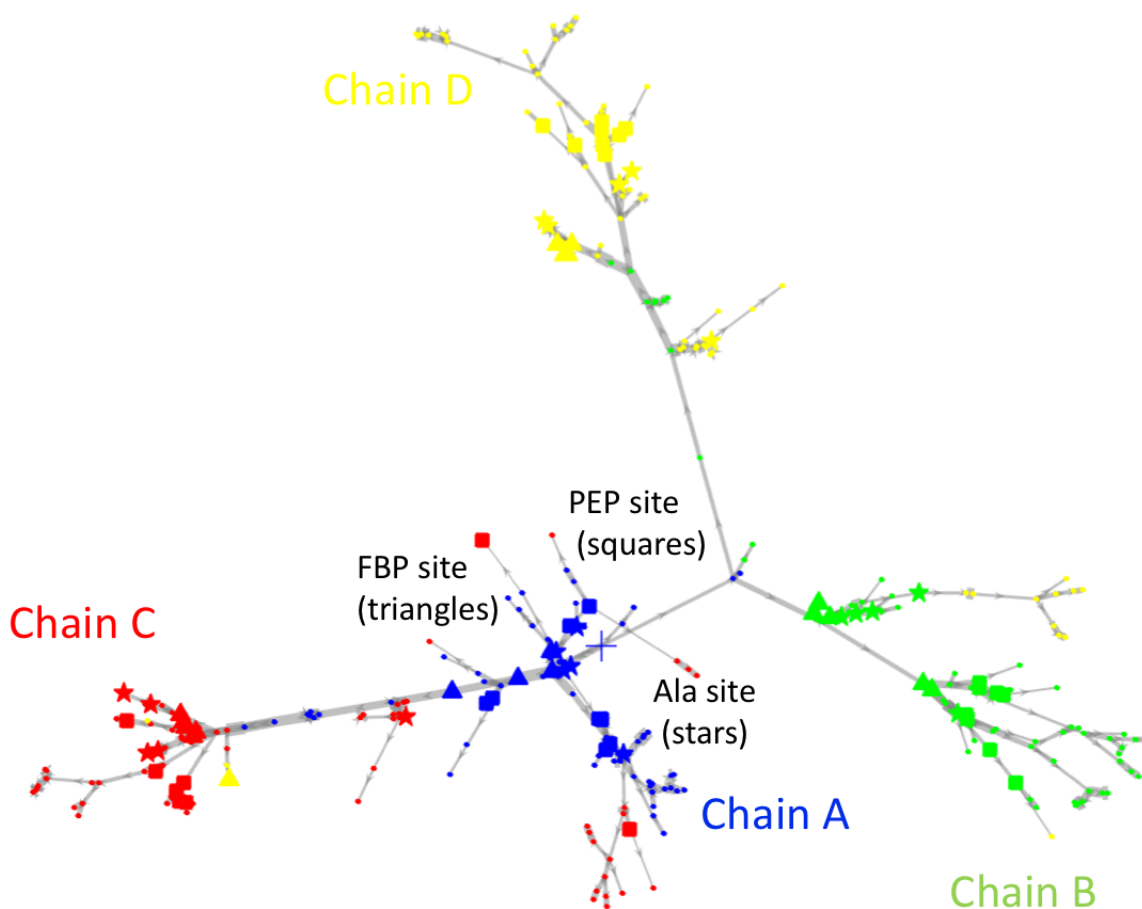
Figure S4. Shortest path tree of mechanical coupling network showing interaction of the chain A FBP site (blue triangles) with all other secondary structural elements in the proteins. Chains are colored; secondary structural elements in PEP sites are shown as squares, FBP sites as triangles, and Ala^E sites as stars. The origin of the search (SSE 85 in the FBP site in Chain A) is shown as a large plus (+). The strength of the coupling is represented by the thickness of lines in between the chain A FBP site is strongly coupled with the PEP and alanine sites on Chain A, with some coupling to the FBP site on chain B and the PEP site on chain C with much longer paths required to reach any other sites.

Comparison of χ and |Q| for Ala^E

A comparison of cost-weighted betweenness centrality parameters and alanine scan results for Ala^E as a ligand, analogous to the comparison shown for FBP in Figure 5, is shown below, with data averaged over secondary structural elements. While the quantitative, residue-by-residue comparison shown in Figure S5 is of similar quality to the comparison observed for FBP, the quality of the visual comparison is reduced by coarse-graining due to the higher degree of locality (e.g. single residue) for mutations affecting Ala^E than for FBP, as mentioned in the main text. Several key regions influencing are identified by the χ analysis of mechanical coupling; these regions are indicated with black arrows on the lower panel of the figure.
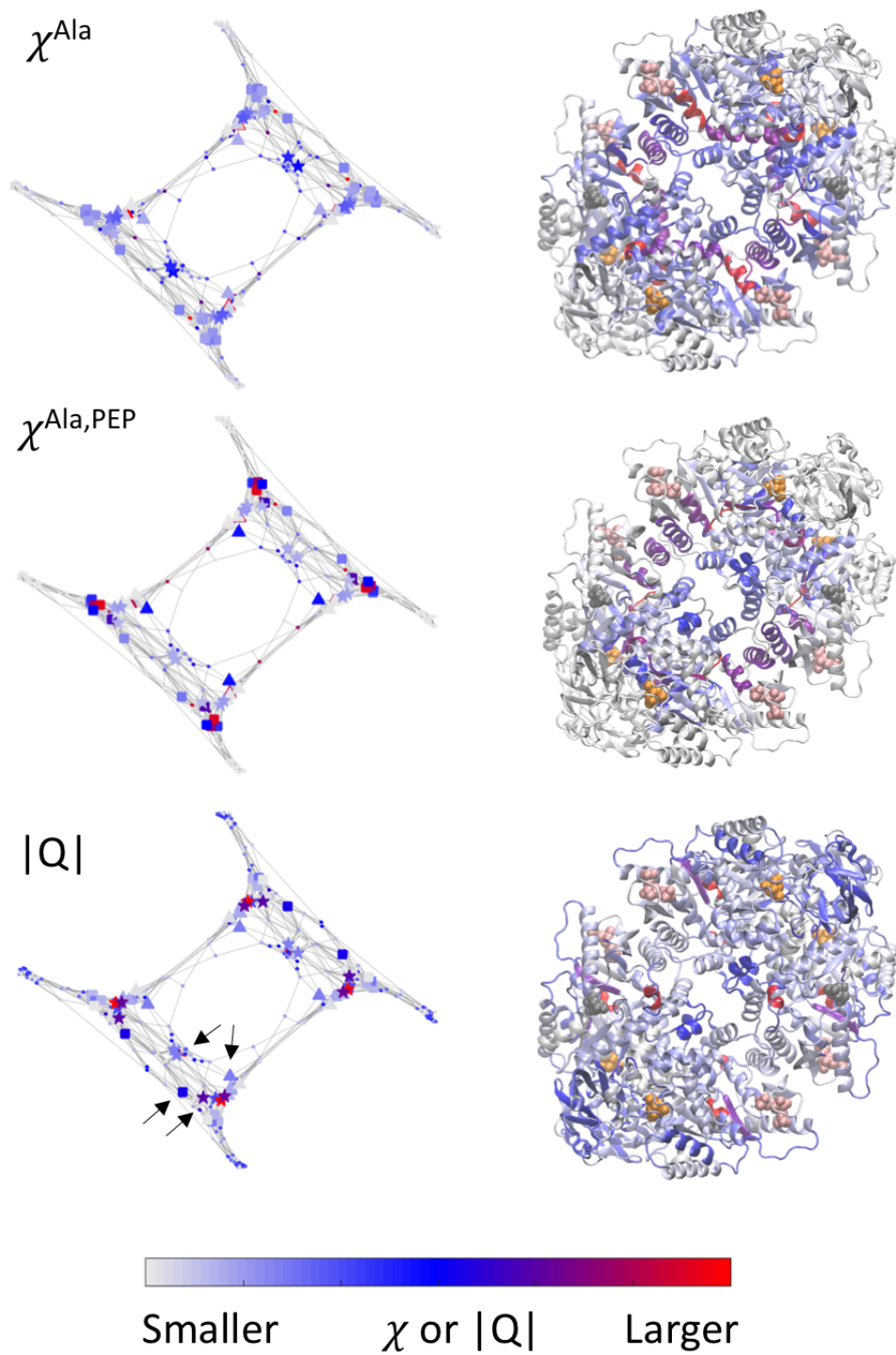
Figure S5. Comparison of χ^{Ala}, $\chi^{\text{Ala,PEP}}$, and |Q| for hL-PYK, averaged over secondary structural elements.

Relationship between FBP and Ala^E allostery

In pyruvate kinase, FBP functions as an allosteric activator of PEP affinity and Ala^E as an allosteric inhibitor of PEP affinity. Of the residues identified by the alanine scan as key to each allosteric effect, some show effects of opposite sign for each ligand, indicating that they are involved in both pathways. The complementarity between allosteric effects is shown in Figure S6.
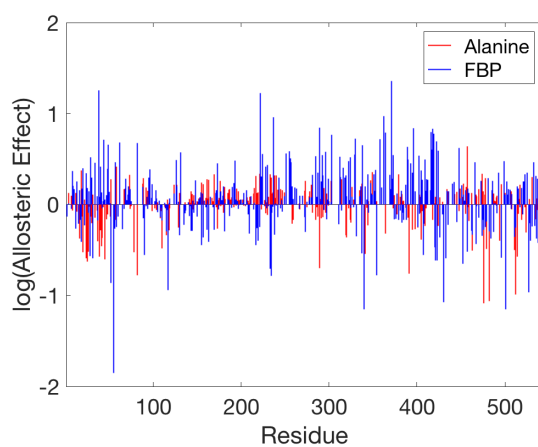
Figure S6. Allosteric effect as represented by alanine scan Q_i/Q_0 for Ala and FBP by residue, showing complementarity between mutations that change the negative allosteric effect of alanine with those that change the positive allosteric effect of FBP.

References for Supporting Information:

1. Proctor, E. A.; Kota, P.; Aleksandrov, A. A.; He, L.; Riordan, J. R.; Dokholyan, N. V., Rational Coupled Dynamics Network Manipulation Rescues Disease-Relevant Mutant Cystic Fibrosis Transmembrane Conductance Regulator. *Chem Sci* **2015,** *6*, 1237-1246. doi:10.1039/C4SC01320D
2. Dokholyan, N. V., Controlling Allosteric Networks in Proteins. *Chem Rev* **2016,** *116*, 6463-6487. doi:10.1021/acs.chemrev.5b00544